# Numerical studies of optical dephasing in ruby

Huang, Shihua; Szabo, Alexander



**Publisher's version / Version de l'éditeur:**
https://doi.org/10.1016/0022-2313(96)00029-4
*Journal of Luminescence, 68, 6, pp. 291-297, 1996-07*

REVISED

# Numerical Studies of Optical Dephasing in Ruby

Shihua Huang† and Alex Szabo

Institute for Microstructural Sciences
National Research Council of Canada
Ottawa, Ontario K1A 0R6, Canada

## ABSTRACT

Computer simulation studies of $^{27}Al$ nuclear spin flip induced dephasing of $R_1$ optical transitions in ruby are presented. Non-exponential echo intensity decays of the form $I = I_0 \exp-(4t/T_m)^x$ were obtained. Good agreement between experimental and theoretical $T_m$'s was obtained for transitions with spin $S_g = -1/2$ and $S_g = -3/2$ in the ground state assuming a nearest neighbour flip rate of 20 kHz. However calculated x values differed from experiment by ~15% for $S_g = -3/2$ and by ~45% for $S_g = -1/2$. Possible limitations of the simulation are discussed in the light of these disagreements.

## 1. Introduction

The concept of a "dephasing time" $T_2$ in low temperature optical solids originally arose from the phenomenological optical Bloch equation (OBE) description[1,2] of two level atoms irradiated with resonant light. In this model, the photon echo intensity I decays exponentially as $I = I_0\exp(-4t/T_2)$. This description was supported in the first[3] and later[4] studies of optical echoes in ruby, in which an exponential decay over four orders of magnitude was observed. However later work with $Pr^{3+}$:$LaF_3$[5] and ruby[6] showed that the OBE did not describe other aspects of optical interaction properly, in particular the optical saturation behaviour and that modifications to the Bloch model were necessary. Several theories were developed[7] showing considerable improvement in describing experiments[5,6] on the power dependence of hole-burning. However more recent studies of time[8,9] and frequency domain[10] phenomena show that the modified OBE do not account for the experiments in a consistent way. Thus there remains a need for further theoretical studies.

Many of the above difficulties are well known from earlier studies in magnetic resonance and are nicely summarized in the classic article by Mims[11]. A common source of dephasing, both for optical and magnetic resonances in solids, is magnetic fluctuations at the impurity site due to nuclear spin flipping in the host lattice and/or electron spin flipping of the dopant ion. In ruby, where both nuclear ($^{27}Al$) and electron ($Cr^{3+}$) spins are present, experiment has shown[12] that for a moderate magnetic field (< 5kG) and for concentrations as low as 0.0023 at%, dephasing primarily arises from indirect[11,12] electron spin flipping, i.e. from magnetic field fluctuations at the (optically resonant) $Cr^{3+}$ site caused by mostly non-resonant flipping $Cr^{3+}$ spins. Also the decay was found to be exponential for $Cr^{3+}$ concentrations in the range 0.0023 to 0.07 at.%. However, calculations[11] using various statistical models show that, in general, spin flip induced echo decay is expected to be non-exponential having a temporal form

$$I = I_0\exp-(4t/T_m)^x \qquad (1)$$

where x can vary from 1/2 to 3 depending on the assumed model.

Because of the complexity of having two spin systems in ruby, an interesting question is: would the decay still be exponential in the absence of Cr-Cr spin flips? To achieve this experimentally, the most obvious approach is to reduce the $Cr^{3+}$ concentration, however this has the difficulty of reduced signal strength. Another idea is to redistribute the spin population into predominantly one level by optical pumping[13] and thereby reduce $Cr^{3+}$spin flips. However the efficacy of this scheme is limited by inhomogeneous broadening[14]. Recently[15,16] another approach has been to work at high fields (> 20kG) and low temperatures (~ 2K), thereby essentially depleting the population of all but the lowest ground state spin level ($S_g$= -3/2). These experiments as well as a later one[17] involving the $S_g$ = - 1/2 spin level have shown a non-exponential decay of the form of Eq. 1 with x, T values of 2.4, 50 usec for $S_g$ = - 3/2 and corresponding values of 2.0, 130 usec for $S_g$ = - 1/2. An attempt was made to analyze the latter observations using a sudden jump model[17] however the results were dependent on assumptions about the size of the frozen core. Because of the complexity of the problem, most theories of spin induced dephasing can be considered only order of magnitude estimates as emphasized by Mims[11]. Also as discussed by DeVoe et al.[18], the theories do not properly account for the lattice structure near the impurity ion and a numerical simulation becomes necessary. Such simulations have recently been extended to several rare earth systems[19-20] which also exhibit non-exponential photon echo decay at high fields.

In this paper we describe numerical simulations of spin flip induced optical dephasing for ruby for both the $^4A_2(-1/2) \rightarrow \overline{E}(-1/2)$ (hereafter $R_1(-1/2)$) and the $R_1(-3/2)$ optical transitions of $Cr^{3+}$ in ruby and compare the results with recent experiments. Only dephasing due to $^{27}Al$ nuclear spin flipping is considered.

2. Description of Model

We consider the magnetic field (optical frequency) fluctuations at a $Cr^{3+}$ site in ruby produced by pairwise flipping of $^{27}Al$ nuclear spins. Typically the fluctuations are calculated for 10,000 time slots of 0.5 to 1 usec. The echo decay is calculated from such a frequency history. The sequence of calculations is:

(1) calculate the spin flip rate of each $^{27}Al$ nucleus with its nearest 26 neighbours out to 1100 $^{27}Al$ nearest the $Cr^{3+}$ ion. The "frozen core" effect, i.e. the detuning of the $^{27}Al$ frequencies from their bulk values by the $Cr^{3+}$ dipolar magnetic field is specifically considered.

(2) a lattice of $^{27}Al$ spins is set up around the $Cr^{3+}$ with spin direction randomly pointing up or down in the field. The applied field is along the c axis and a spin I = 1/2 for $^{27}Al$ is assumed.

(3) optical frequency fluctuations of the $Cr^{3+}$ are calculated using an algorithm for following the spin flipping sequences.

(4) randomly selected small time intervals from the total history of ~10 msec are used to calculate the echo decay. Usually 10,000 intervals representing the frequency history of 10,000 $Cr^{3+}$ were chosen.

The mutual spin flip rate is given by Fermi's golden rule as

$$W_{ij} = W_0 r_0^6 (1 - 3\cos^2\theta_{ij})^2 r_{ij}^{-6} \Gamma^2 (\Gamma^2 + D_{ij}^2)^{-1} \qquad (2)$$

where $r_{ij}$ is the distance between atoms i and j, $\theta_{ij}$ is the angle between $\vec{r}_{ij}$ and the magnetic field, $\Gamma$ is the bulk nuclear linewidth (HWHM) and $D_{ij}$ is the difference between the i'th and j'th resonance optical frequencies. Also $r_0$ is the distance between the nearest $^{27}Al$ and $4W_0$ is the corresponding flip rate for $^{27}Al$'s far from the $Cr^{3+}$ ion ($D_{ij} = 0$). In the calculation of $D_{ij}$, only the dipolar term of

the $^{27}Al$ spin Hamiltonian[22,23] was considered. Exchange and quadrupolar terms were neglected. Calculations where these terms were included indicated little (<5%) effect on the echo decay parameters $T_m$ and x. The essential reason for this is that the first shell of 13 $^{27}Al$'s surrounding the $Cr^{3+}$ has a very slow flip rate and has little effect on the decay dynamics as will be demonstrated later. We note also that for a large (>20 kG) field along the c axis, the Zeeman term in the nuclear spin Hamiltonian is dominant resulting in almost pure spin states. This means that the magnetic field change due to pairwise $^{27}Al$ flipping is independent of the assumed nuclear spin because of the flip selection rule, $\Delta I_1 = \pm 1/2$, $\Delta I_2 = \mp 1/2$.

The detuning factor $D_{ij}$ is given by

$$D_{ij} = \gamma_n (H_i - H_j)/(2\pi) \tag{3}$$

where $\gamma_n$ is the $^{27}Al$ nuclear gyromagnetic ratio, $H_{i,j}$ is the c axis component of the $Cr^{3+}$ dipolar field at the $^{27}Al$ sites i and j. The wavefunction of a $Cr^{3+}$ ion in an optical superposition state is given by $|\psi> = a|G>|S_g> + b|E>|S_e>$ where G, E are ground and excited state electronic wavefunctions and $|S>$ is a spin wavefunction. The expectation value of the magnetic moment $<\mu> = <gS>$ is $aa^* g_g <S_g> + bb^* g_e <S_e> = [(1-w)g_g <S_g> + (1+w)g_e <S_e>]/2$ where w is the population component of the Bloch vector. The c axis component of the magnetic field at the i'th $^{27}Al$ site due to the $Cr^{3+}$ dipolar field is given by

$$H_i = <\mu>\beta(1-3\cos^2\theta_i)r_i^{-3} \tag{4}$$

where $r_i$ is the distance from the $Cr^{3+}$ to the i'th $^{27}Al$ and $\theta_i$ is the angle between the c axis and $\vec{r}_i$. For weakly excited echoes, $w \approx -1$ and $H_i$ is mainly determined by the ground state values. However for an optimal $\pi/2$, $\pi$ excitation sequence, w = 0 and both ground and excited state parameters will determine the size of the frozen core and hence the echo decay.

Two spin flip simulation algorithms were studied. In the fast algorithm (FA), spin flipping for each $^{27}Al$ is followed in turn over 10,000 time slots, and the changes in spin orientations along with the frequency shifts recorded. Clearly the time sequencing of this procedure is incorrect. For the slow algorithm(SA), all 1100 $^{27}Al$'s are followed in parallel through each time step. This results in a 1100× longer calculation (~ 11 hrs. on a HP382 computer using compiled Basic). Essentially identical results were obtained with both algorithms and hence the FA was used for simulations.

The FA proceeds by calculating a flip time $t_{ij} = -\ln(R_j)/W_{ij}$ for the i'th $^{27}Al$ with its 26 neighbours (j = 1 to 26). $R_j$ is a random number in the range 0 to 1.A flip only can occur for spins of opposite orientations. For each time interval, the spin with the smallest $t_{ij}$ is assumed to flip and the change in spin orientation and the $Cr^{3+}$ frequency change is recorded. The process is then restarted for the next time interval. After all time intervals have been completed, the calculation is repeated for each of the 1100 $^{27}Al$ sites.

For the calculation of echo decay from a frequency history, two algorithms were studied. In one, many histories (corresponding to different $Cr^{3+}$'s) were used to calculate the echo intensity from

$$I(T) = I_0 \left| \sum_{j=1}^{N} \exp[i\phi_j(2T)] \right|^2 \tag{6}$$

where

$$\phi_j(2T) = \sum_{n=0}^{T/t_0} 2\pi[f_j(t_n + T) - f_j(t_n)]t_0 \tag{7}$$

In Eq. 6 and 7, T is the time span over which the echo decay is followed, $f_j$ is the frequency of the j'th Cr, $t_0$ is the time slot length, N is the number of $Cr^{3+}$ and n is the time slot number. In algorithm 2, the frequency history of one $Cr^{3+}$ is calculated for an extended time period (typically

10 to 30 msec). Then pieces of this decay are randomly selected corresponding to the number of $Cr^{3+}$ (usually 10,000) to use in Eq. 7. Because the process is ergodic, the two methods gave essentially identical results and all calculations presented used algorithm 2 which was easier to implement. Finally we note that the number of ions N determines how many orders of decay are simulated. Since the emitted intensity is ~ $N^2$ at zero time when all dipoles are coherent and ~ N at times longer than the dephasing time, the asymptote of the decay curve is expected to be a factor ~ N below the starting point. Calculations have generally confirmed this argument.

The parameters used in the calculations are $g_g$=1.984,$g_e$=2.445, $\beta$=1.40 MHz/G, $\gamma_n=2\pi\times1.1$ kHz/G, $\Gamma$ = 3.0 kHz, $r_0=2.733\times10^{-8}$ cm, w=-1 and $W_0$ = 5000 $sec^{-1}$.

3. Results

Fig. 1 shows the $^{27}$Al spin flip rate dependence on the magnetic field change at the $Cr^{3+}$ site due to pairwise flips of the $^{27}$Al's. Interestingly, the rates are seen to fall on well defined curves, each of which corresponds to a particular lattice site (or set of three because of trigonal symmetry) in the first or second shell of $^{27}$Al's surrounding a given $^{27}$Al. The first shell contains 4 sets of 3 equivalent atoms (labeled I,J,K,L[22,23]) and the G, N atoms located along the c axis immediately above and below the atom in question. The G atom (spaced by $r_0$) is closest and flips the fastest. The flip rate of first shell atoms J and L is ~ 10× slower than that of the more distant second shell atoms P, P', R. The reason for this is that they are located near the "magic angle" given by $\cos\theta = 1/\sqrt{3}$. Thus spin diffusion tends to proceed mainly parallel (via G and N atoms) and nearly perpendicular (via the I atoms) to the c axis. The frozen core character is evident in that near the $Cr^{3+}$, the flip rate decreases and the magnetic field change, $\Delta H$, increases. As we go farther from the $Cr^{3+}$ and out of the frozen core, the flip rate increases and $\Delta H \rightarrow 0$.

Fig. 2 shows calculated echo decays for the $R_1(-1/2)$ and $R_1(-3/2)$ transitions along with fits to the equation $I/I_0=\exp(-4t/T_m)^x$ with $T_m$ and x as parameters. The results for the two algorithms discussed earlier are nearly the same.

The effect of excitation pulse intensity, via it's effect on the Bloch population vector w, is shown in Fig. 3. For weak pulses, $w \rightarrow -1$.

Fig. 4 shows the effect of removing $^{27}$Al's nearest to the Cr ion. Removal of the first and second shell of $^{27}$Al's (~ 100 atoms) has a small effect on the echo parameters, confirming the existence of a "frozen core" as discussed earlier. Finally Fig. 5 and 6 show the effect of variation of the nuclear linewidth and nearest neighbour flip rate on the echo parameters which will be discussed further in the next section.

## 4. Discussion

We consider pump intensity effects as determined by different frozen core sizes in the ground and excited states. (This intensity dependence is distinct from "instantaneous diffusion" which involves interaction between the echo [24] or related [25] ions.) In Fig. 3, $T_m$ is seen to lengthen for $R_1(-1/2)$ and shorten for $R_1(-3/2)$ as w increases from -1 to +1. For the former, this is due to the increase in average core size because of the larger g value of $Cr^{3+}$ in the excited state while for the latter, it is due to the decrease in average core size arising from the smaller excited state electron spin. Since the $^{27}$Al flip rates near the $Cr^{3+}$ vary inversely with core size, the $T_m$ are correspondingly affected. We note in passing, that although $R_1(-3/2)$ has a larger frozen core[23] than $R_1(-1/2)$ in the ground state, the former has a shorter $T_m$ because of it's much larger (~ 7.6×) magnetic splitting factor[26]. The intensity dependence of echo decay predicted by the above considerations has not been observed experimentally[16] however perhaps a wider range of intensity needs study. The distribution of w for finite width excitation pulses will diminish the intensity dependence, however it will not have a major effect if pulsewidths $\ll T_m$ are used.

Experimental parameter values for the $R_1(-1/2)$ and $R_1(-3/2)$ transitions in dilute ruby are shown in Fig. 7. From Fig. 2, we see good agreement between calculated and experimental $T_m$ values at high fields assuming $W_0$=5000 $sec^{-1}$. However the experimental x values differ considerably from the simulation.

A theoretical value of $W_0$ can be derived[20] from a discussion by Abragam[27], assuming a Lorentzian lineshape for the dipolar broadened $^{27}Al$ nuclear spin transition. The nearest neighbour flip rate in the bulk, $4W_0$, is given by

$$4W_0 = \frac{\hbar^2 \gamma_n^4 r_0^{-6}}{4\pi\Gamma} \tag{8}$$

Using the bulk nuclear linewidth (HWHM) $\Gamma$=3 kHz and $\gamma_n/(2\pi)$=1.1 kHz/Gauss in Eq. 1 gives $W_0$=42 $sec^{-1}$, which is some two orders of magnitude smaller than that required to fit the experimental data. This discrepancy is, we believe, related to the question of the nature of the $^{27}Al$ dipolar broadened linewidth. As discussed by Mims[11] and Abragam[28], the broadening due to dipolar interactions is inhomogeneous on a time scale comparable to the spin flip time. Two-thirds of a dipolar broadened line is "static" and one-third is "dynamic", the latter arising from direct and indirect flip-flop terms $I^+I^-$ in the interaction Hamiltonian. Near the $Cr^{3+}$, these ratios change considerably. For example a lower limit of 20 for the ratio of inhomogeneous to homogeneous width for $^{27}Al$'s in the first shell has been observed[12]. These considerations complicate the flip rate calculation in Eq. 1 since not only must the homogeneous width be used, but the position of the resonance within the inhomogeneous line must be modeled by calculation of the fields both due to $Cr^{3+}$ electron spin and $^{27}Al$ nuclear spins. Obviously such a calculation would require considerable computing resources.

If we assume that the bulk $^{27}$Al dephasing time[29] $T_2$=60 usec is determined completely by direct spin flips, then from Eq. 1, we have

$$T_f^{-1} = W_0 r_0^6 \sum_i (1-3\cos^2\theta_{ij})^2 r_{ij}^{-6} \tag{9}$$

where the spin flip time $T_f$ is related to $T_2$ by $T_2$=2 $T_f$, since $T_f$ is a lifetime limiting process similar to $T_1$. The lattice sum is $1.7895\times10^{46}$ cm$^{-6}$ giving $W_0$=4450 sec$^{-1}$, which is near the experimental value. While this is a gratifying result, it may be simply fortuitous in light of the above discussion.

In conclusion, the presented numerical simulation of dephasing of optical $R_1$ transitions in ruby semi-quantitatively describes the non-exponential photon echo decay in dilute ruby at high fields, in particular the relative values of the echo parameter, $T_m$. The x echo parameter was found to be essentially independent of non spatial parameters such as Bloch population vector (Fig. 3), nuclear linewidth (Fig. 5), nearest neighbour flip rate (Fig. 6) and ground state spin. It seems likely that x will depend on the spatial correlations of $^{27}$Al spins. We note that earlier work[12] has suggested the correlations are different for $S_g$ = -1/2 and -3/2 spins. This difference may be responsible for the different x values observed for the $R_1$(-1/2) and $R_1$(-3/2) transitions.

## 5. Acknowledgement

The expert technical assistance of J. Froemel in the experiments is gratefully acknowledged.

†Changchun Institute of Physics, Chinese Academy of Sciences, Changchun 130021, China.

References

1. R.P. Feynman, F.L. Vernon Jr. and R.W. Hellwarth, J. Appl. Phys. 22 (1957) 49.
2. L. Allen and J.H. Eberly in "Optical Resonance and Two-Level Atoms", (J. Wiley, New York, 1975) p.26.
3. N.A. Kurnitt, I.D. Abella and S.R. Hartmann, Phys. Rev. Lett. 15 (1964) 567.
4. S. Meth and S.R. Hartmann, Phys. Lett. 58A (1976) 192.
5. R.G. DeVoe and R.G. Brewer, Phys. Rev. Lett. 50 (1983) 1269.
6. A. Szabo and T. Muramoto, Phys. Rev. A39 (1989) 3992.
7. P.R. Berman, J. Opt. Soc. Am. B3 (1986) 564 and references therein.
8. T. Muramoto and A. Szabo, Phys. Rev. A38 (1988) 5928.
9. R.N. Shakhmuratov and A. Szabo, Phys. Rev. B48 (1993) 6903.
10. A. Szabo and R. Kaarli, Phys. Rev. B44 (1991) 12307.
11. W.B. Mims in "Electron Paramagnetic Resonance", edited by S. Geschwind, (Plenum Press, New York, 1972) p.263.
12. A. Szabo, T. Muramoto and R. Kaarli, Phys. Rev. B42 (1990) 7769.
13. A. Szabo and J. Heber, Phys. Rev. A29 (1984) 3452.
14. P.E. Jessop and A. Szabo in "Laser Spectroscopy V', eds. A.R.W. McKellar, T. Oka and B.P. Stoicheff (Springer-Verlag, Heidelberg, 1981) p. 408.
15. J. Ganen, Y.P. Wang, R.S. Meltzer and W.M. Yen, Phys. Rev. B10 (1991) 8599.
16. J. Ganen, Y.P. Wang, D. Boye, R.S. Meltzer, W.M. Yen, R. Wannemacher and R.M. Macfarlane, Phys. Rev. Lett. 66 (1991) 695.
17. A. Szabo, J. Lumin. 58 (1994) 403.
18. R.G. DeVoe, A. Wokaun, S.C. Rand and R.G.Brewer, Phys. Rev. 23 (1981) 3125.
19. R.M. Macfarlane, R. Wannemacher, D. Boye, Y.P. Wang and R.S. Meltzer, J. Lumin. 48 & 49 (1991) 313.
20. R.S. Meltzer, J. Ganen, Y.P. wang, D. Boye, W.M. Yen, D.P. Landau, R. Wannamacher and R.M. Macfarlane, J. Lumin. 53 (1992) 1.

21. R.S. Meltzer and D.P. Landau in "Computer Simulation Studies in Condensed Matter Physics V", (Springer-Verlag, Berlin, 1993) p.191.

22. S. Meth and S.R. Hartmann, Otp. Comm. 24 (1978) 100.

23. A. Szabo, J. Opt. Soc. Amer. B3 (1986) 514.

24. J. Huang, J.M. Zhang, Z. Lezama and T.W. Mossberg, Phys. Rev. Lett. 63 (1989) p.78.

25. M. Mitsunaga, T. Takagahara, R. Yano and N. Vesugi, Phys. Rev. Lett. 68 (1992) 3216.

26. A. Szabo, Opt. Lett. 8 (1983) 486.

27. A. Abragam. The Principles of Nuclear Magnetism (Oxford, London, 1961) p.137-8.

28. ref. 27, p.112.

29. R. Boscaino, F.M. Gelardi and R.N. Mantega, Phys. Lett. 103A (1984) 391.

Figure Captions

Fig. 1: Dependence of the magnetic field change at the $Cr^{3+}$ site on the $^{27}Al$-$^{27}Al$ spin flip rates for a lattice of 1100 $^{27}Al$'s. $^{27}Al$ atom designations as in ref. 22 and 23. Type G atoms are closest, lying along the c axis. Atom sets I,J,K,L are in the first shell, the remainder are in the second shell of $^{27}Al$'s surrounding a given site.

Fig. 2: Simulation of photon echo decay for the (a) $R_1(-1/2)$ and (b) $R_1(-3/2)$ transitions in ruby using the long (x) and short (o) algorithms discussed in the text. The solid line is a fit to the decay equation $I=I_0\exp(-4t/t_m)^x$ using the indicated values. $W_0$=5000 $sec^{-1}$ is assumed.

Fig. 3: Excitation intensity dependence of echo decay parameters. w is the Bloch population component (w = -1 for the ground state).

Fig. 4: Calculated echo parameter dependence on the number of $^{27}Al$ removed from lattice, starting from those nearest the Cr.

Fig. 5: Calculated echo parameter dependence on the bulk nuclear linewidth.

Fig. 6: Calculated echo parameter dependence on the nearest neighbour spin flip rate, $4W_0$.

Fig. 7: Experimental echo parameter dependence on magnetic field for the (a) $R_1(-1/2)$ [ref. 17] and (b) $R_1(-3/2)$ transitions in ruby. Cr concentration = 0.0023 at%, temperature = 2.2K.

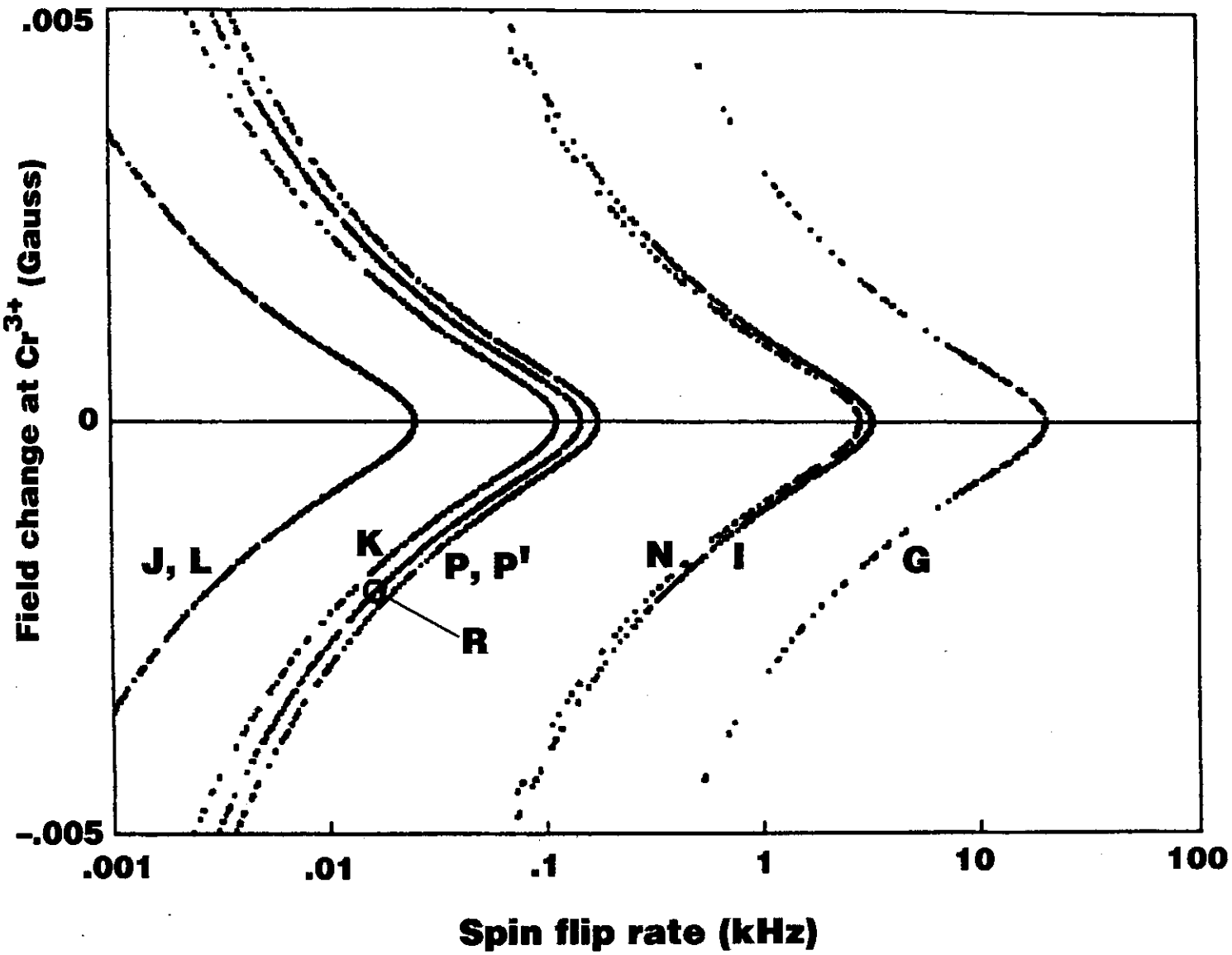
.005
0
-.005
Field change at $Cr^{3+}$ (Gauss)
.001
.01
.1
1
10
100
Spin flip rate (kHz)
J, L
K
P, P'
R
N
I
G

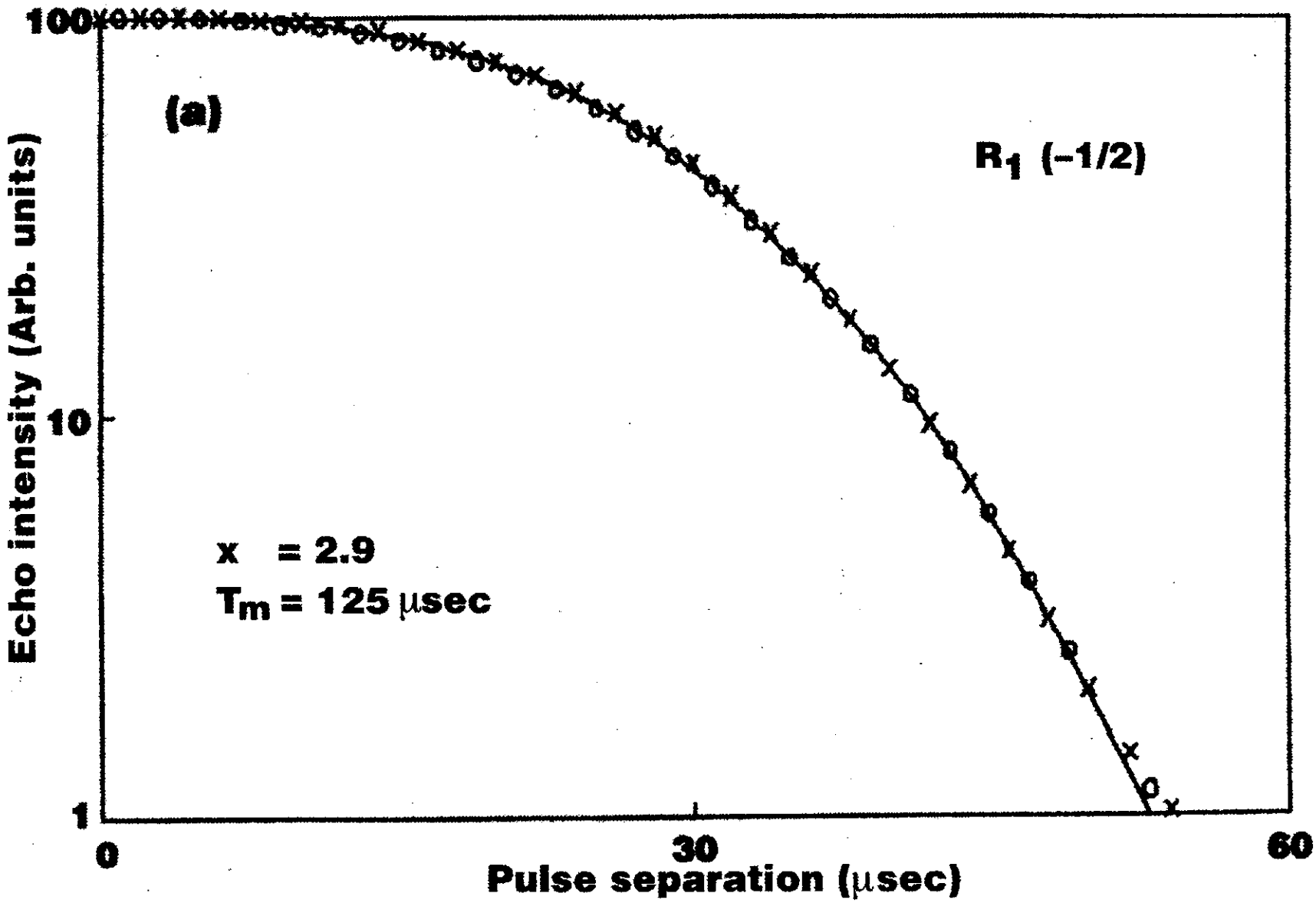
(a)
R1 (-1/2)
x = 2.9
Tm = 125 μsec
Echo intensity (Arb. units)
100
10
1
0
30
60
Pulse separation (μsec)

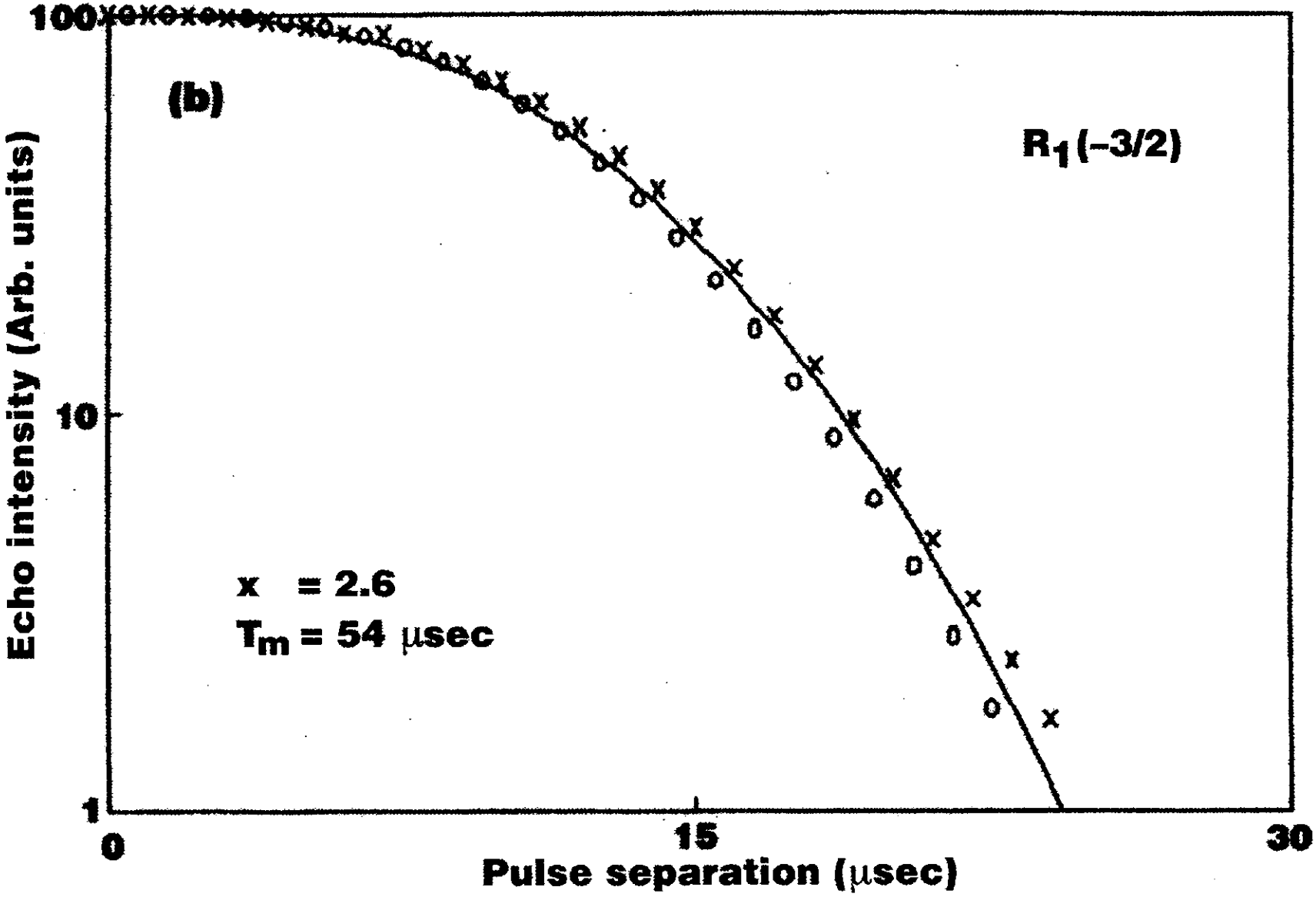
(b)
$R_1(-3/2)$
x = 2.6
$T_m$ = 54 μsec
Echo intensity (Arb. units)
100
10
1
0
15
30
Pulse separation (μsec)

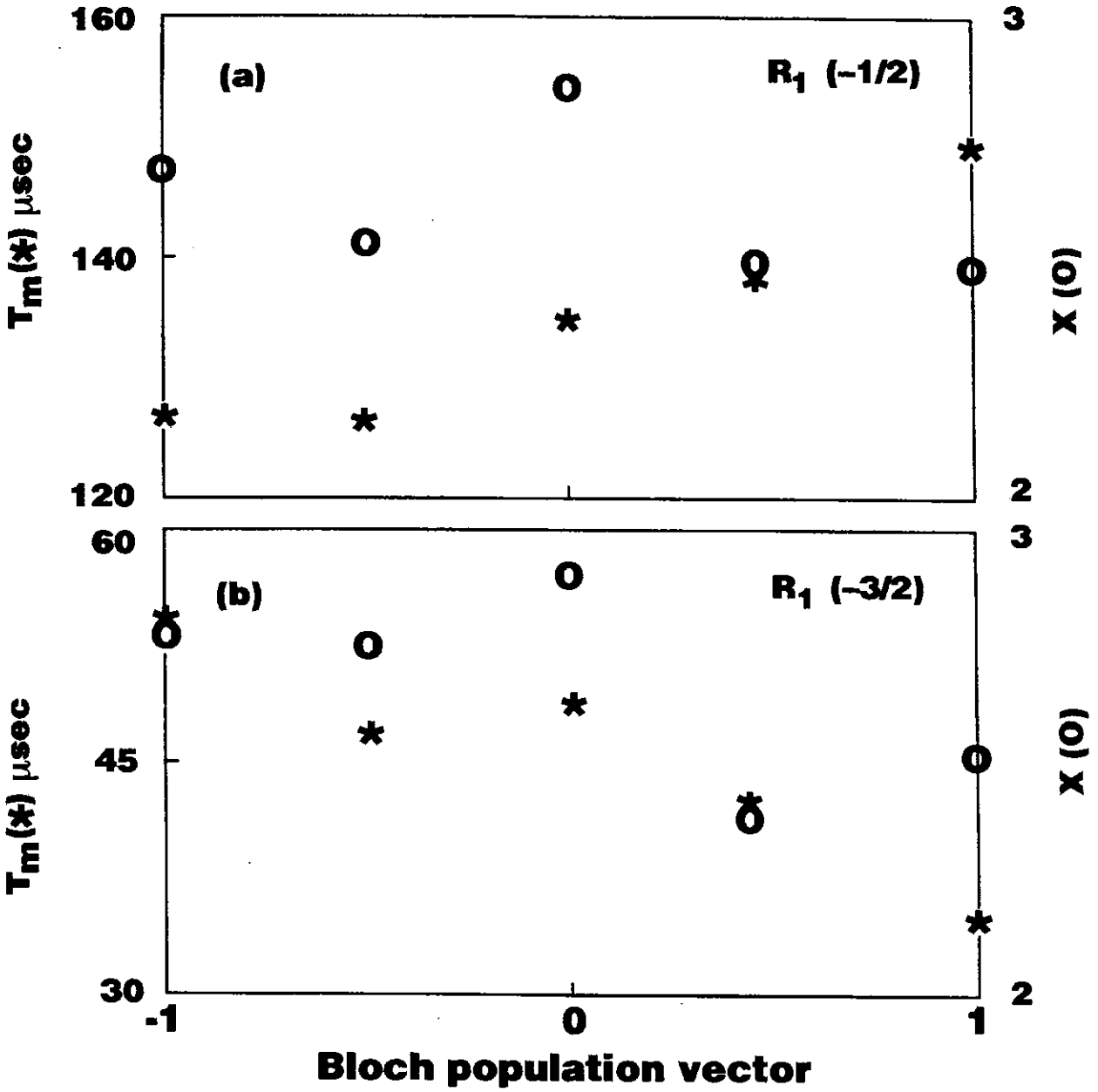
160
140
120
(a)
R1 (-1/2)
Tm(*) μsec
X (O)
3
2
60
45
30
(b)
R1 (-3/2)
-1
0
1
Bloch population vector

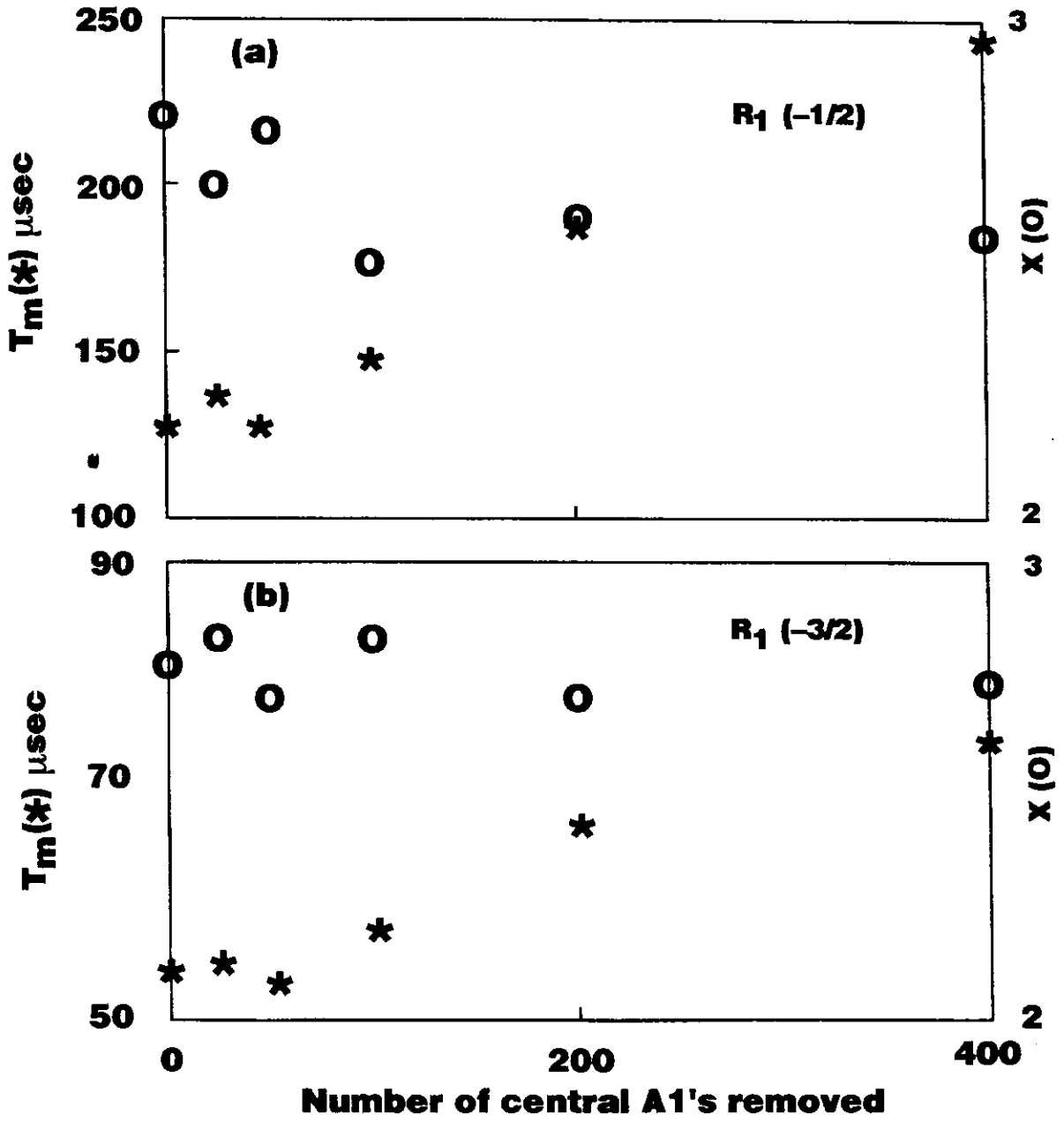
(a)
R1 (-1/2)
250
200
150
100
3
2
Tm(*) μsec
X (O)
(b)
R1 (-3/2)
90
70
50
3
2
Tm(*) μsec
X (O)
0
200
400
Number of central A1's removed

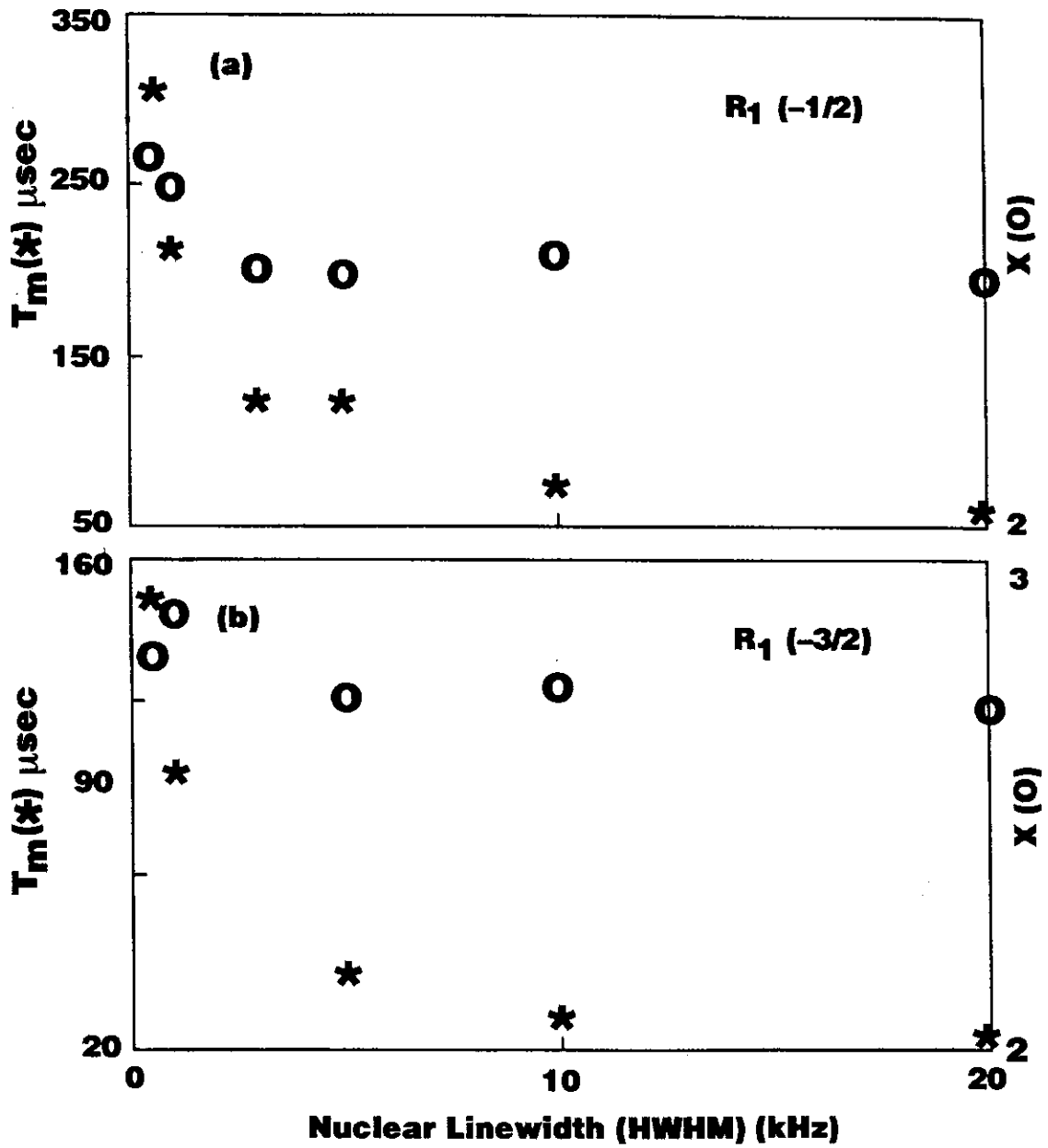
(a)
R1 (-1/2)
Tm(*) μsec
X (O)
350
250
150
50
2
(b)
R1 (-3/2)
160
90
20
3
2
0
10
20
Nuclear Linewidth (HWHM) (kHz)

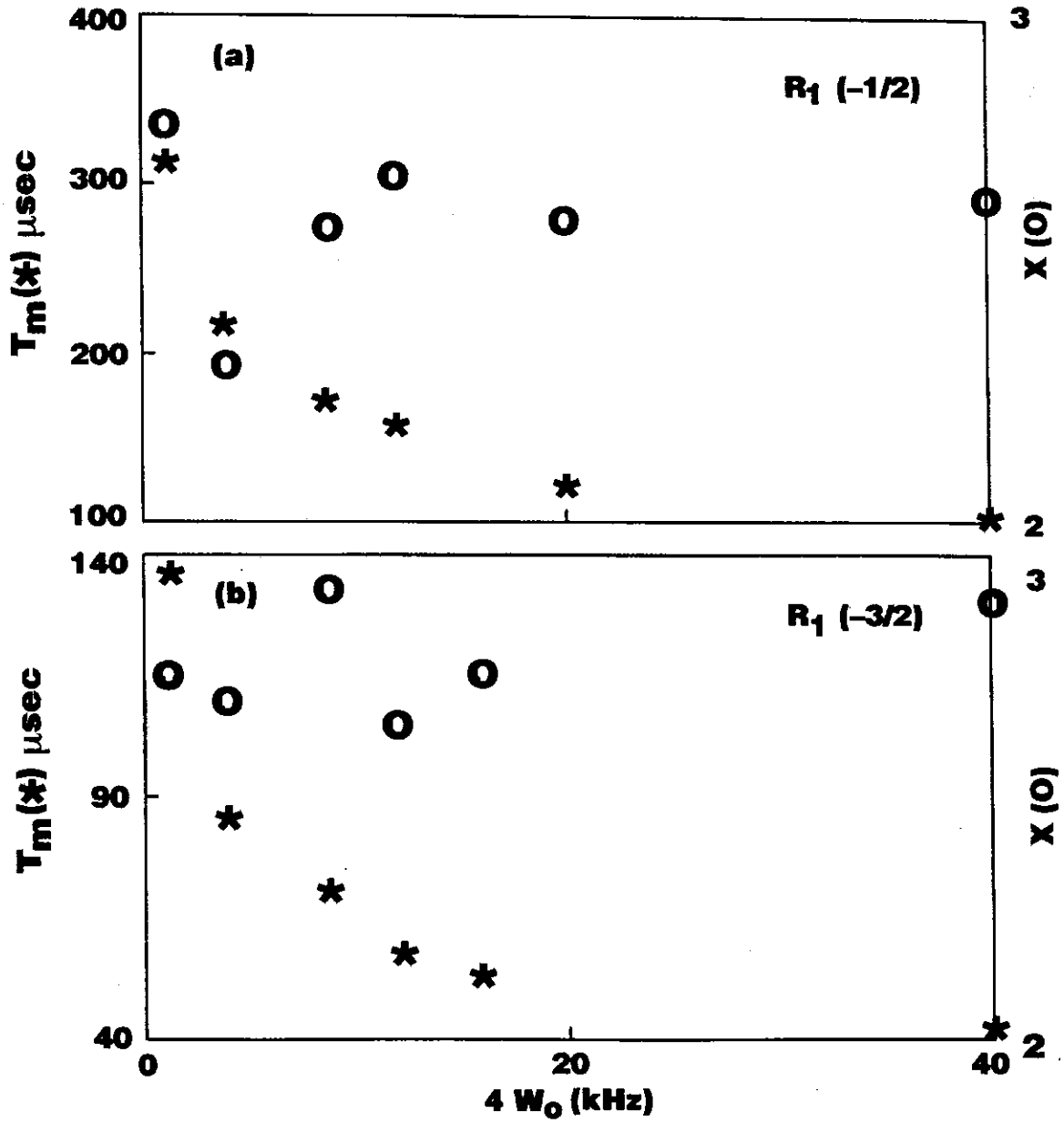
(a)
R1 (-1/2)
400
300
200
100
3
2
Tm(*) μsec
X (O)
(b)
R1 (-3/2)
140
90
40
3
2
Tm(*) μsec
X (O)
0
20
40
4 Wo (kHz)

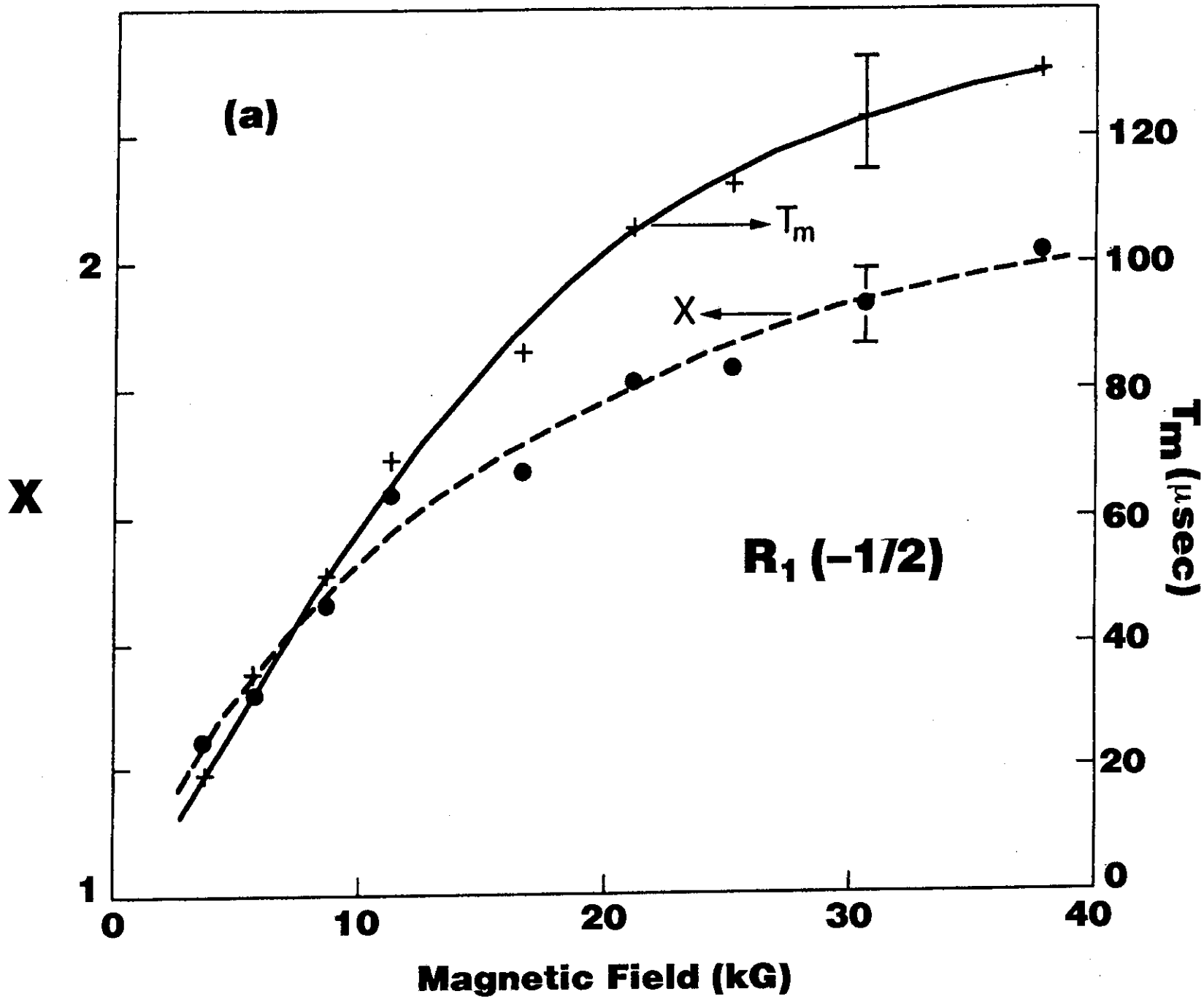
(a)
X
2
1
0
10
20
30
40
Magnetic Field (kG)
120
100
80
60
40
20
0
Tm (μsec)
Tm
X
R1 (−1/2)

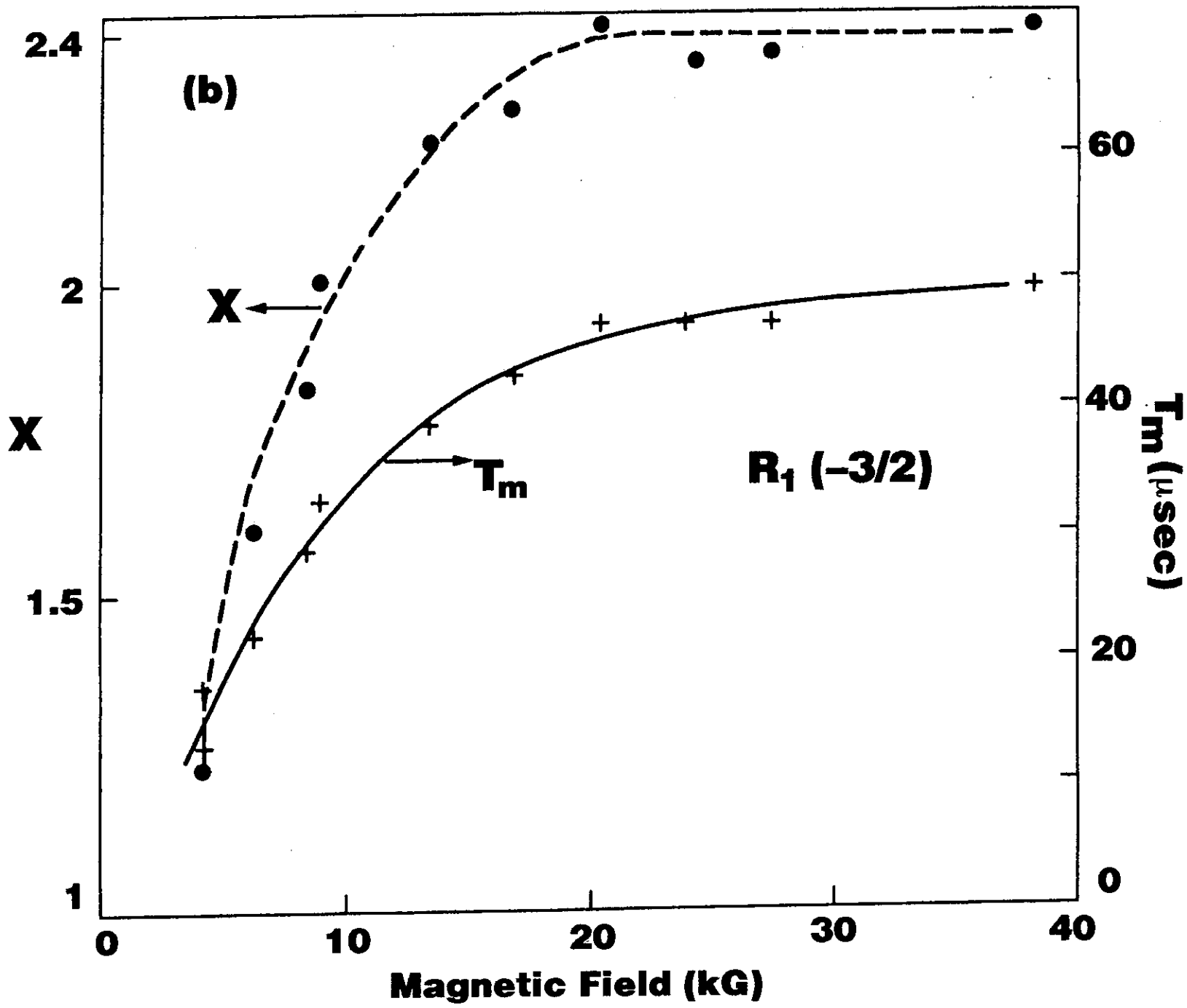
(b)
X
$T_m$
$R_1$ (−3/2)
X
$T_m$ (μsec)
Magnetic Field (kG)
2.4
2
1.5
1
60
40
20
0
0
10
20
30
40